
CYClE: Chosing Your Collorators Wisely to Enhance Collaborative Fairness in Decentralized Learning

Nurbek Tastan
MBZUAI
nurbek.tastan@mbzuai.ac.ae

Samuel Horváth
MBZUAI
samuel.horvath@mbzuai.ac.ae

Karthik Nandakumar
MBZUAI, MSU
karthik.nandakumar@mbzuai.ac.ae

Abstract

Collaborative learning (CL) enables multiple participants to jointly train machine learning (ML) models on decentralized data sources without raw data sharing. While the primary goal of CL is to maximize the expected accuracy gain for each participant, it is also important to ensure that the gains are **fairly** distributed. Specifically, no client should be negatively impacted by the collaboration, and the individual gains must ideally be commensurate with the contributions. Most existing CL algorithms require central coordination and focus on the gain maximization objective while ignoring collaborative fairness. In this work, we first show that the existing measure of collaborative fairness based on the correlation between accuracy values without and with collaboration has drawbacks because it does not account for negative collaboration gain. We argue that maximizing mean collaboration gain (MCG) while simultaneously minimizing the collaboration gain spread (CGS) is a fairer alternative. Next, we propose the CYClE protocol that enables individual participants in a private decentralized learning (PDL) framework to achieve this objective through a novel reputation scoring method based on gradient alignment between the local cross-entropy and distillation losses. Experiments on the CIFAR-10, CIFAR-100, and Fed-ISIC2019 datasets empirically demonstrate the effectiveness of the CYClE protocol to ensure positive and fair collaboration gain for all participants, even in cases where the data distributions of participants are highly skewed. For the simple mean estimation problem with two participants, we also theoretically show that CYClE performs better than standard FedAvg, especially when there is large statistical heterogeneity.

1 Introduction

Collaborative learning (CL) refers to a framework where several entities can work together by pooling their resources to achieve a common machine learning (ML) objective without sharing raw data. This approach offers particular advantages in domains like healthcare and finance that require access to extensive datasets, which can be difficult to acquire for any single entity due to the costs involved or privacy regulations such as HIPAA [3] and GDPR [10]. Federated learning (FL) [19] is a specific case of CL that enables multiple entities to collectively train a shared model by sharing their respective model parameters or gradients with a central server for aggregation. However, FL methods can lead to information leakage associated with sharing gradients/parameter updates with an untrusted

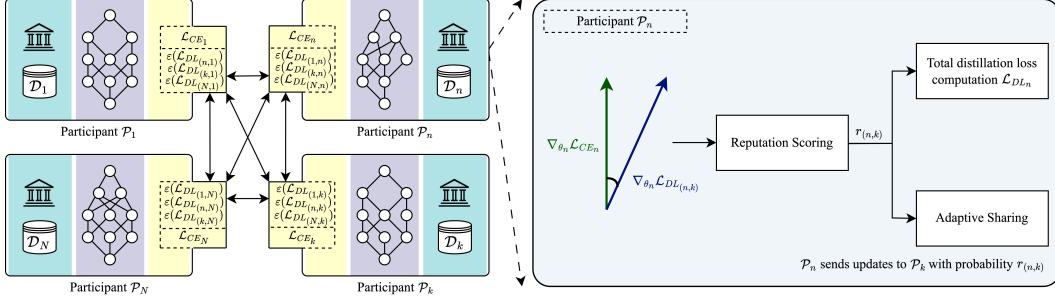


Figure 1: Illustration of the proposed Choose Your Collaborators Wisely (CYCLe) protocol for Private Decentralized Learning (PDL).

third-party server that can potentially carry out reconstruction attacks [32, 30]. Furthermore, most CL algorithms assume that all participating agents are contributing equally to the learning process. When this assumption is violated, there is little incentive for collaboration because the gains are not distributed fairly. To avoid these pitfalls, a fully decentralized learning algorithm that fairly rewards the contributions of individual participants is required.

Recent works have attempted to tackle the challenge of *collaborative fairness* (CF) in FL settings. Shapley value (SV) [22] is often used to estimate marginal utility of participants in FL. However, computing the SV involves high computation and communication costs. To mitigate this problem, variants of SV have been proposed in [26, 16, 28]. But these methods only focus on FL with a central server. Existing private decentralized learning (PDL) algorithms such as CaPriDe [25], CaPC [7], and Cronus [4] emphasize on confidentiality, privacy and utility, while ignoring collaborative fairness.

In this work, we aim to bridge this significant gap by designing the CYCLe protocol for knowledge sharing in the PDL setting. We focus on three goals - maximizing the mean accuracy gain across all participants, ensuring that no participant suffers performance degradation due to collaboration, and the accuracy gains are evenly distributed. To achieve these goals, we make the following contributions:

- We analyze the *collaborative fairness metric* based on correlation coefficient between the contributions of participants and their respective final accuracies, and show that it fails in cases where the collaboration gain is negative.
- We introduce the *CYCLe protocol* that regulates knowledge transfer among participants in a PDL framework based on their reputations to achieve better collaborative fairness. The proposed *reputation scoring* scheme uses gradient alignment between cross-entropy and distillation losses to accurately assess relative contributions made by collaborators in PDL.
- We theoretically study the CYCLe protocol in the context of mean estimation between two participants and show that it outperforms FedAvg in the presence of data heterogeneity.

2 Related Work and Background

Several challenges associated with CL have been addressed recently, including privacy [8, 7, 4, 25, 14, 9, 20], confidentiality [25, 7, 4], communication efficiency [19], robustness [17, 1, 2], and fairness [28, 31, 24, 18]. Most existing works focus only on FL algorithms with central orchestration such as FedAvg [19]. Due to the potential harm caused by gradient leakage in FL [30, 32], which can result in the disclosure of sensitive user data, there is a growing interest in decentralized learning algorithms that do not require centralized orchestration. Focus has been mainly on ensuring confidentiality, privacy, and utility in decentralized learning [25, 7, 4].

To achieve collaborative fairness in CL, it is critical to evaluate marginal contributions of participants [12, 28, 23, 13]. The main reason to have a robust data valuation technique is the heterogeneous nature of data distribution across clients, meaning that some clients may contribute more useful data than others. In vanilla FL, all participants receive the same global model irrespective of their contributions, which can potentially discourage collaboration and increase resistance to practical adoption. While Shapley Value (SV) can be used for data valuation, SV computation is expensive and hard to employ [22]. In CGSV [28], cosine similarity between local and global parameter updates is

used to approximate the SV. The same cosine similarity approach is used in RFFL [27] for reputation scoring. Kumar et al. [16] used logistic regression models as proxies for client data and utilized an ensemble of them to approximate the SVs.

2.1 Preliminaries

Notations: Let $\tilde{\mathcal{M}}_\theta : \mathcal{X} \rightarrow \mathcal{Y}$ be a supervised classifier parameterized by θ , where $\mathcal{X} \subseteq \mathbb{R}^d$ and $\mathcal{Y} = \{1, 2, \dots, M\}$ denote the input and label spaces, respectively, d is the input dimensionality, and M is the number of classes. Let $\mathcal{M}_\theta : \mathcal{X} \rightarrow \mathcal{Z}$ denote a mapping from the input to the logits space ($\mathcal{Z} \subset \mathbb{R}^M$) and σ_T be a softmax function (with temperature parameter T) that maps the logits into a probability distribution $\mathbf{p} = \sigma_T(\mathbf{z})$ over the M classes. The sample is eventually assigned to the class with the highest probability. Given an input sample $\mathbf{x} \in \mathcal{X}$ and its ground truth label $y \in \mathcal{Y}$, let \mathcal{L}_{CE} denote the cross entropy (CE) loss based on the prediction $\sigma_T(\mathcal{M}_\theta(\mathbf{x}))$ and y . We denote $\mathcal{L}_{DL(i,j)}$ as the pairwise distillation loss between two models \mathcal{M}_{θ_i} and \mathcal{M}_{θ_j} . For example, the distillation loss (DL) could be computed as KL divergence between $\sigma_T(\mathcal{M}_{\theta_i}(\mathbf{x}))$ and $\sigma_T(\mathcal{M}_{\theta_j}(\mathbf{x}))$. Note that other types of distillation losses [11] can also be used in lieu of KL divergence.

Decentralized Learning: Let N be the number of collaborating participants and $\mathcal{N} = \{1, 2, \dots, N\}$. We assume that each participant $\mathcal{P}_n, n \in \mathcal{N}$ has its own local training dataset \mathcal{D}_n and a hold-out validation set $\tilde{\mathcal{D}}_n$. Based on the local training set, each participant can learn a local ML model \mathcal{M}_{θ_n} by minimizing the local cross entropy loss \mathcal{L}_{CE_n} . The validation accuracy of this standalone local model \mathcal{M}_{θ_n} on $\tilde{\mathcal{D}}_n$ is denoted as \mathcal{B}_n . The goal in a typical FL algorithm is to build a single global model \mathcal{M}_{θ_g} that has a better accuracy than the standalone accuracy of all the local models. In contrast, the goal of each participant in decentralized learning is to obtain a better local model $\mathcal{M}_{\theta_n^*}$, which has a higher local validation accuracy \mathcal{A}_n after collaboration. In other words, each participant \mathcal{P}_n aims to maximize its *collaborative gain* (CG), which is defined as $\mathcal{G}_n = (\mathcal{A}_n - \mathcal{B}_n)$. This is typically achieved by minimizing the following objective:

$$\mathcal{L}_n = \mathcal{L}_{CE_n} + \lambda_n \mathcal{L}_{DL_n}, \quad (1)$$

where \mathcal{L}_{DL_n} denotes the total distillation loss of \mathcal{P}_n and $\lambda_n > 0$ is a hyperparameter that controls the relative importance of the cross entropy and distillation losses. Note that the term DL in the above formulation is used generically (without restricting to any specific loss function) and it intuitively captures the differences between the local model of a participant and the models of all its collaborators. The total DL of \mathcal{P}_n can in turn be computed by aggregating the pairwise distillation losses as follows:

$$\mathcal{L}_{DL_n} = \sum_{k \in \mathcal{N} \setminus \{n\}} \lambda_{(n,k)} \mathcal{L}_{DL(n,k)}, \quad (2)$$

where $\mathcal{L}_{DL(n,k)}$ is the pairwise DL between \mathcal{P}_n and \mathcal{P}_k and $\lambda_{(n,k)}$ are the weights assigned to the pairwise losses between different participants.

Private Decentralized Learning (PDL): In the PDL framework, the total DL is computed in a privacy-preserving way without leaking the local data of participants. For example, CaPC learning [7] leverages secure multi-party computation, homomorphic encryption, and differential privacy (DP) to securely estimate \mathcal{L}_{DL_n} . However, CaPC learning requires a semi-trusted third-party privacy guardian to privately aggregate local predictions and the pairwise distillation losses are not accessible. In contrast, CaPriDe learning [25] utilizes fully homomorphic encryption (FHE) to securely compute an approximation of the pairwise DL losses. However, all existing PDL algorithms lack a mechanism to assess the contributions of different participants within the CL framework. Hence, $\lambda_{(n,k)}$ is usually set to $\frac{1}{(N-1)}$ and $\lambda_n = \lambda_0, \forall n \in \mathcal{N}$. λ_0 is typically determined through hyperparameter search. We refer to the above scenario as *vanilla PDL* (VPDL).

3 Towards a Better Fairness Metric

In [18, 27], collaborative fairness (CF) is defined as follows:

Definition 1. In a federated system, a high-contribution participant should be rewarded with a better performing local model than a low-contribution participant. Mathematically, fairness can be quantified by the correlation coefficient between the contributions of participants and their respective final model accuracies. [18]

In the above CF Definition 1, the contribution of a participant is typically evaluated based on its standalone local accuracy (\mathcal{B}_n). Thus, the CF metric attempts to ensure that participants with higher standalone accuracy receive a model with higher final accuracy (\mathcal{A}_n) compared to that received by other participants. However, the problem with this approach can be illustrated using a simple example. Consider two participants \mathcal{P}_1 and \mathcal{P}_2 with standalone accuracy of 60% and 80%, respectively. Suppose that after collaboration, \mathcal{P}_1 (\mathcal{P}_2) receives a model with an accuracy of 70% (70.1%). In this scenario, the system is considered perfectly fair (with a fairness measure of 1) according to the above CF definition, because \mathcal{P}_2 receives a model with higher accuracy compared to \mathcal{P}_1 . However, it is obvious that only \mathcal{P}_1 benefits from this collaboration and achieves a CG of $\mathcal{G}_1 = 10\%$, whereas \mathcal{P}_2 gains nothing. Strictly speaking, \mathcal{P}_1 has a negative CG of $\mathcal{G}_2 = -9.9\%$, but it can always dump the collaboratively trained model and use its own standalone model to achieve zero CG. This scenario cannot be considered as fair, because the participant with the lower contribution benefits significantly without helping the participant with higher contribution.

The problem with CF quantification in Definition 1 is that it overlooks the scenario where the collaboration gain is negative. This is usually not the case in FL with iid settings, because all the participants have similar standalone accuracy and the accuracy of the collaboratively learned model is much higher than any of the individual standalone accuracies. However, in extreme non-iid settings (which is where collaborative fairness is most needed!), the problem of negative CG can be encountered often. Hence, there is a need for a better metric to quantify collaborative fairness.

One possible solution is to measure the rewards in terms of CG, instead of the final model accuracies. Consequently, fairness can be quantified by the correlation coefficient between the contributions of participants (\mathcal{B}_n) and their respective collaboration gains (\mathcal{G}_n). However, the drawback of this approach is that it is inherently much harder to improve the performance of the higher contribution participant who starts with a much higher standalone accuracy. Going back to the earlier example, if \mathcal{P}_1 improves from 60% to 70%, \mathcal{P}_2 has to improve its accuracy from 80% to more than 90% to achieve a fairness score of 1. While it is much easier to satisfy the first condition, it is hard to meet the second condition using any CL algorithm. Hence, the fairness metric based on the correlation between standalone accuracy and CG is likely to be negative for most cases, indicating poor fairness.

A better alternative is to minimize the probability that the CG is negative or zero, i.e., $P(\mathcal{G}_n \leq 0)$ should be small. Intuitively, this is possible only when the expected value (μ) of \mathcal{G}_n is a large positive value and if the standard deviation (ν) of \mathcal{G}_n is small. Mathematically, using the well-known Chebyshev single-tail inequality, we can show that $P(\mathcal{G}_n \leq 0)$ is bounded by $\frac{\nu^2}{\nu^2 + \mu^2} = \frac{1}{(1 + (\mu/\nu)^2)}$, provided $\mu > 0$. Thus, minimizing $P(\mathcal{G}_n \leq 0)$ requires maximizing μ and minimizing ν . Let the mean collaboration gain (MCG) and collaboration gain spread (CGS) be defined as the sample mean and standard deviation of CG across participants, i.e.,

$$\text{MCG} = \frac{1}{N} \sum_{n=1}^N \mathcal{G}_n, \quad \text{CGS} = \sqrt{\frac{1}{(N-1)} \sum_{n=1}^N (\mathcal{G}_n - \text{MCG})^2}. \quad (3)$$

Hence, an ideal decentralized learning scheme should maximize MCG (achieve better utility), while at the same time minimize CGS (ensure that all participants benefit fairly). This minimizes the likelihood of a participant being negatively impacted by the collaboration (having negative CG).

4 Proposed CYCLe Protocol

Assumptions and Scope: In this work, we restrict ourselves to the PDL framework presented in Eqs. 1 and 2. We also assume a cross-silo setting, where the number of participants is relatively small ($N < 10$) to ensure practical feasibility of PDL. Our method requires a PDL algorithm that can compute pairwise DL in a privacy-preserving way. While we employ CaPriDe learning [25] as the baseline method for PDL in this work, other alternatives can also be used. Complete description of the baseline PDL method and discussions about its convergence, communication efficiency, or privacy guarantees are beyond the scope of this work.

Rationale: To maximize its individual CG (and hence maximize MCG), each participant must intuitively give more importance to distillation losses corresponding to other reliable participants, while de-emphasizing distillation losses corresponding to unreliable participants. To minimize CGS, each participant must penalize other unreliable participants (who do not contribute to its own learning)

by sharing less knowledge with them. To achieve both these goals, we need to solve the following two sub-problems: (i) **Reputation Scoring** (RS): How to efficiently evaluate the reliability/reputation $r_{(n,k)}$ of participant \mathcal{P}_k in the context of collaborative learning of model \mathcal{M}_{θ_n} belonging to \mathcal{P}_n ?, (ii) **Adaptive Sharing** (AS): How to regulate knowledge transfer among participants based on the reputation score to achieve collaborative fairness?.

4.1 Reputation Scoring

Several reputation scoring methods have been proposed in the FL literature [27, 15, 29]. These reputation scores are generally used by the FL server either for client selection or for weighted aggregation. In contrast to FL, where a global model is learned by a central server, each participant builds its own local model in PDL. Hence, it is not possible to compute a single reputation score for a PDL participant. Instead, each participant has its own local estimate of the reputation of other participants. Hence, the same participant may be assigned different reputation scores by its collaborators.

The proposed reputation scoring is based on the intuition that gradient alignment between the local CE loss and pairwise DL is a strong indicator of the utility of \mathcal{P}_k to \mathcal{P}_n . For example, if the two gradients are completely misaligned (either because the data distributions of the \mathcal{P}_k and \mathcal{P}_n do not have any overlap or because \mathcal{P}_k is malicious), attempting to learn from \mathcal{P}_k is likely to harm the learning of \mathcal{P}_n , rather than being beneficial. On the other hand, if there is perfect alignment, the two gradients reinforce each other and accelerate the model learning at \mathcal{P}_n . In fact, if KL divergence is used for pairwise DL computation, the gradients based on the local CE loss and pairwise DL will be closely aligned only when the predictions made \mathcal{P}_k on \mathcal{P}_n 's data closely match the ground-truth labels available with \mathcal{P}_n . This is because the CE loss measures the ‘‘distance’’ between $\sigma_T(\mathcal{M}_{\theta_n}(\mathbf{x}))$ and y , while the DL loss measures the ‘‘distance’’ between $\sigma_T(\mathcal{M}_{\theta_n}(\mathbf{x}))$ and $\sigma_T(\mathcal{M}_{\theta_k}(\mathbf{x}))$. These two losses will lead to aligned gradients only when $\sigma_T(\mathcal{M}_{\theta_k}(\mathbf{x}))$ is close to y . This justifies our choice of using gradient alignment between CE loss and pairwise DL as the basis for reputation scoring.

The reputation of a participant \mathcal{P}_k from the perspective of \mathcal{P}_n (denoted as $r_{(n,k)}$) is computed in two steps. First, the gradient (mis)alignment metric $s_{(n,k)}$ is computed as:

$$s_{(n,k)} = \frac{1 - \cos(\nabla_{\theta_n} \mathcal{L}_{CE_n}, \nabla_{\theta_n} \mathcal{L}_{DL_{(n,k)}})}{2}, \quad (4)$$

where $\nabla_{\theta_n} \mathcal{L}_{CE_n}$ and $\nabla_{\theta_n} \mathcal{L}_{DL_{(n,k)}}$ are the gradients of cross entropy and distillation losses, respectively, with respect to the current parameters θ_n of participant \mathcal{P}_n , $n \in \mathcal{N}$, and $k \in \mathcal{N} \setminus \{n\}$. Note that $s_{(n,k)} \rightarrow 0$ indicates better gradient alignment. We empirically observed that when gradient alignment $s_{(n,k)}$ is below a threshold τ_{opt} , collaboration with \mathcal{P}_k is mostly beneficial to \mathcal{P}_n . This is because as long as the predictions of \mathcal{P}_k are closer to the ground-truth at \mathcal{P}_n , learning from \mathcal{P}_k will help \mathcal{P}_n . In contrast, when $s_{(n,k)}$ is above a threshold τ_{max} , collaboration with \mathcal{P}_k becomes harmful to \mathcal{P}_n . Based on these observations, we compute the reputation score by applying a soft clipping function to $s_{(n,k)}$. Specifically, the reputation score in the current round $\tilde{r}_{(n,k)} = h(s_{(n,k)})$, where h is defined as:

$$h(s) = \max\left(0, \min\left(1, \frac{s - \tau_{max}}{\tau_{opt} - \tau_{max}}\right)\right) \quad (5)$$

Algorithm 1 CYCLe ($t, k, \nabla_{\theta_n} \mathcal{L}_{CE_n}$)

Input: Hyperparameters $\alpha, \tau_{opt}, \tau_{max}, \lambda_0$

```

1:  $\phi \leftarrow$  Is Update Available from  $\mathcal{P}_k$ ?
2: Reputation Scoring
3: if  $\phi = 0$  then
4:    $\mathcal{L}_{DL_{(n,k)}} \leftarrow 0$ 
5: else
6:    $\mathcal{L}_{DL_{(n,k)}} \leftarrow$  Get DL from  $\mathcal{P}_k$ 
7:   if  $(t \bmod R) = 0$  then
8:      $s \leftarrow \frac{1 - \cos(\nabla_{\theta_n} \mathcal{L}_{CE_n}, \nabla_{\theta_n} \mathcal{L}_{DL_{(n,k)}})}{2}$ 
9:      $\tilde{r} \leftarrow h(s)$ 
10:     $r_{(n,k)}^t \leftarrow \alpha r_{(n,k)}^{t-1} + (1 - \alpha)\tilde{r}$ 
11:   end if
12: end if
13: Adaptive Sharing
14: if  $(t \bmod R) = 0$  then
15:   Share predictions with  $\mathcal{P}_k$ 
16: else
17:    $z \leftarrow$  Uniform( $[0, 1]$ )
18:   if  $z \leq r_{(k,n)}$  then
19:     Share predictions with  $\mathcal{P}_k$ 
20:   end if
21: end if
22: return  $(r_{(n,k)}^t, \mathcal{L}_{DL_{(n,k)}})$ 

```

To minimize variations due to stochasticity, the reputation score is updated using a momentum factor, i.e., $r_{(n,k)}^t = \alpha r_{(n,k)}^{(t-1)} + (1 - \alpha)\tilde{r}_{(n,k)}$, where $0 < \alpha < 1$ is the momentum hyperparameter and $r_{(n,k)}^t$ is the final reputation score in round t ($t > 0$). When $t = 0$, $r_{(n,k)}^t = \tilde{r}_{(n,k)}$. Henceforth, we drop the index t for convenience. A higher reputation score $r_{(n,k)}$ implies that updates from \mathcal{P}_k are useful for model learning at \mathcal{P}_n . Hence, \mathcal{P}_n can directly utilize $r_{(n,k)}$ to weight ($\lambda_{(n,k)}$) the pairwise distillation loss. While it is possible to perform reputation scoring and dynamically update the weights $\lambda_{(n,k)}$ after every collaboration round, it can also be performed periodically (after a fixed number of rounds) to minimize computational costs.

Algorithm 2 Private Decentralized Learning (PDL) based on Proposed CYCLe Protocol

Input: Number of participants N , maximum communication rounds t_{max} , and learning rate η

Assumption: Each \mathcal{P}_n has $\mathcal{D}_n = \{\mathbf{x}_{j,n}, y_{j,n}\}_{j=1}^{|\mathcal{D}_n|}$

```

1:  $\mathcal{M}_{\theta_n^0} \leftarrow$  Local training at  $\mathcal{P}_n, \forall n \in \mathcal{N}$ 
2: for each round  $t = 0, 1, \dots, t_{max}$  do
3:   for each participant  $n \in \mathcal{N}$  do
4:      $\mathcal{L}_{CE_n} \leftarrow$  Compute cross-entropy loss of  $\mathcal{P}_n$ 
5:      $\nabla_{\theta_n} \mathcal{L}_{CE_n} \leftarrow$  Compute the gradient of  $\mathcal{L}_{CE_n}$ 
6:     for each participant  $k \in \mathcal{N} \setminus \{n\}$  do
7:        $(r_{(n,k)}^t, \mathcal{L}_{DL(n,k)}) \leftarrow$  CYCLe( $t, k, \nabla \mathcal{L}_{CE_n}$ )
8:     end for
9:      $\lambda_{(n,k)} \leftarrow r_{(n,k)}^t$ 
10:     $\mathcal{L}_{DL_n} \leftarrow \sum_{k \in \mathcal{N} \setminus \{n\}} \lambda_{(n,k)} \cdot \mathcal{L}_{DL(n,k)}$ 
11:     $\mathcal{L}_n \leftarrow \mathcal{L}_{CE_n} + \lambda_0 \cdot \mathcal{L}_{DL_n}$ 
12:     $\theta_n^t \leftarrow \theta_n^{t-1} - \eta \nabla_{\theta_n} \mathcal{L}_n$ 
13:  end for
14: end for

```

4.2 Adaptive Sharing

Once the reputation scores are computed, \mathcal{P}_n can use $r_{(n,k)}$ to choose its collaborators wisely. Specifically, \mathcal{P}_n can decide if it needs “to share or not to share” the distillation loss $\mathcal{L}_{DL(k,n)}$ with \mathcal{P}_k . To be precise, \mathcal{P}_n computes and sends $\mathcal{L}_{DL(k,n)}$ to \mathcal{P}_k with probability $r_{(n,k)}$. This adaptive sharing mechanism plays a key role in ensuring collaborative fairness. In order to receive updates from \mathcal{P}_n in the current collaboration round, participant \mathcal{P}_k needs to maintain a high reputation score with \mathcal{P}_n . This in turn requires sharing of updates that are useful for model learning at \mathcal{P}_n in the previous round.

The above reputation-based adaptive sharing scheme has the following advantages: (1) It incentivizes \mathcal{P}_k to share honest and useful updates with \mathcal{P}_n . Sharing noisy or malicious updates will hurt \mathcal{P}_k ’s reputation score and hence, dampen \mathcal{P}_k ’s ability to learn from \mathcal{P}_n . (2) If \mathcal{P}_n finds that \mathcal{P}_k has a low reputation score, it will send updates less frequently to \mathcal{P}_k , thereby saving valuable computational and communication resources. Note that in the PDL framework, privacy-preserving DL loss computation is often computationally expensive. However, there is one limitation in the proposed protocol. If \mathcal{P}_n is malicious, it can deviate from the protocol and stop sending updates to \mathcal{P}_k even though $r_{(n,k)}$ is high. While this can be addressed by penalizing participants (by reducing their reputation score) for not sharing updates, such an approach is not desirable because it will force participants to keep sharing updates even if they are not benefiting from the collaboration. Hence, we go for a compromise solution, where all the parties are forced to share updates after every R collaboration rounds and the reputation scores are re-calibrated based on these responses.

4.3 Mean Estimation as a Toy Example for CYCLe Protocol

Consider a simple scenario involving two clients, $N = 2$, each aiming to estimate the mean of their data distributions (θ_1 and θ_2) by collaborating using the CYCLe protocol. It can be shown that the probability of the estimate obtained through collaboration being better than a standalone estimate is lower bounded by $(1/8) \exp(-1/4\gamma^2)$, where γ is the variance of the standalone estimate (see Theorem A.1). More importantly, this bound is independent of the data heterogeneity, which contrasts with FedAvg. More details about this analysis are available in the supplementary material.

5 Experiments

Datasets: **CIFAR-10** [15] is a dataset consisting of 60000 images of size 32×32 pixels, categorized into 10 classes with 6000 images per class. It has 50000 training and 10000 test samples. **CIFAR-100** dataset [15] shares similarities with the CIFAR-10 dataset, but it consists of 100 classes with

Table 1: Performance comparison on CIFAR-10 dataset: Validation accuracy evaluated with $N = 5$ participants. The top section of the table presents the performance of our proposed framework compared to the FedAvg algorithm. The bottom part of the table compares collaboration gain and fairness of our proposed CYCLE algorithm with existing works (rows 6-9). We employ MVA (\uparrow), MCG (\uparrow) and CGS (\downarrow) as evaluation metrics.

Setting	Homogeneous			Dirichlet (0.5)			Imbalanced (0.8, 1)			Imbalanced (0.35, 2)			Imbalanced (0.6, 1)		
Metric	MVA	MCG	CGS	MVA	MCG	CGS	MVA	MCG	CGS	MVA	MCG	CGS	MVA	MCG	CGS
FedAvg	90.60	7.20	0.48	88.76	21.40	4.31	90.17	26.35	14.51	90.34	13.12	9.61	90.16	16.28	9.11
VPDL	84.98	1.58	0.71	74.27	6.91	2.31	67.18	3.36	3.58	78.71	1.49	4.01	75.43	1.55	2.45
CYCLE	86.33	2.93	0.32	76.93	9.57	2.07	69.26	5.44	2.56	81.12	3.89	2.65	76.72	2.83	1.38
CFFL	62.65	2.21	0.87	49.04	2.49	2.35	58.66	3.48	4.39	65.08	9.99	9.95	65.20	14.35	9.79
RFFL	61.50	1.05	0.95	48.52	1.96	1.63	56.27	1.08	2.45	58.51	3.43	7.46	51.35	0.50	6.74
CGSV	63.27	2.83	0.94	54.45	7.90	3.40	55.96	0.78	9.32	61.99	6.91	11.34	61.34	10.49	11.23
CYCLE	71.95	11.51	0.58	51.21	4.65	1.11	61.80	6.62	2.79	68.26	13.17	7.12	64.93	14.08	6.22

600 samples per class. The training and test sets are divided in the same way as in CIFAR-10. CIFAR-100 dataset is used with data augmentation (random rotation (up to 15 degrees), random crop, and horizontal flip). **Fed-ISIC2019** [21] (from FLamby benchmark) is a multi-class dataset of dermoscopy images comprising of 23, 247 images with 8 different melanoma classes and high label imbalance (ranging from 49% to less than 1% for class 0 to 7). The dataset is designed for 6 clients based on the centers. Train/test split is: (9930/2483), (3163/791), (2691/672), (1807/452), (655/164), (351/88).

5.1 Experimental Setup

Baseline approaches: We consider several existing FL algorithms as baselines: vanilla FL based on FedAvg (FedAvg) [19], FL based on cosine gradient Shapley value (CGSV) [28], collaborative fairness in FL (CFFL) [18], and robust and fair FL (RFFL) [27]. The above methods are designed for FL with central orchestration. As mentioned earlier, the baseline VPDL method is based on CaPriDe learning [25]. We also evaluate standalone (SA) accuracy, where each participant trains its ML model on its local dataset without any collaboration with others. Furthermore, we report the results for these baseline methods on CIFAR-10 and CIFAR-100.

Participant data splitting strategies: We implement three types of strategies to split the training dataset among the participants: (i) **homogeneous**, (ii) **heterogeneous**, and (iii) **imbalanced dataset sizes** (denoted as ‘imbalanced’). Homogeneous setting refers to the case where each participant gets an equal number of data points per class. In contrast, the heterogeneous method assigns a varying number of data points to each participant, based on a Dirichlet(δ) distribution. The parameter δ reflects the degree of non-IID characteristics within the dataset, where smaller values of δ leads to a more heterogeneous setting, while larger values tend towards an IID setting. To determine the specific allocation, we sample $p \sim Dir_N(\delta)$ and assign a fraction p_n of the total data samples to \mathcal{P}_n . We employ these settings for CIFAR-10 and CIFAR-100 with the following number of participants: $N = 2, 5, 10$. In all our experiments, we utilize all the training samples (e.g. all 50000 samples of CIFAR-10 and CIFAR-100). In the case of the imbalanced data distribution, we utilize a custom function that relies on parameters κ and m , where κ determines the proportion of data points received by each of the m chosen participants. The remaining $(N - m)$ participants then share the remaining data among themselves. We explore this setting with $N = 5$ participants and consider the following

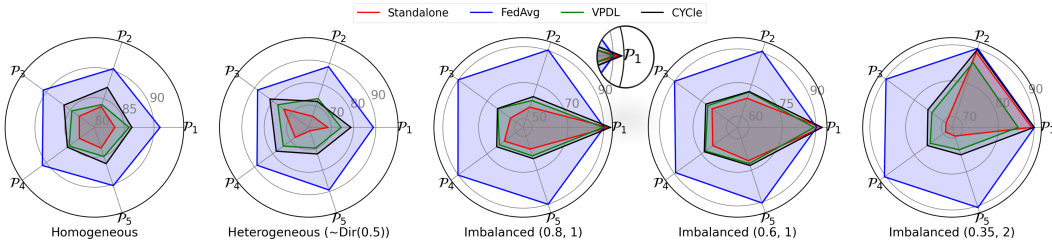


Figure 2: Per-participant performance comparison on CIFAR-10 dataset: Validation accuracy evaluated with $N = 5$ participants.

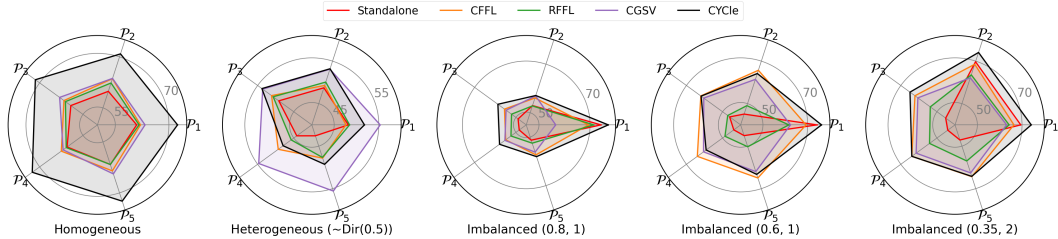


Figure 3: Per-participant performance comparison on CIFAR-10 dataset using custom CNN architecture from [28]: Validation accuracy evaluated with $N = 5$ participants.

configurations: (i) imbalanced ($\kappa = 0.8, m = 1$), (ii) imbalanced ($\kappa = 0.35, m = 2$), and (iii) imbalanced ($\kappa = 0.6, m = 1$). For example, in the last case, one participant holds 60% of the data, while the remaining 4 participants get 10% of the data each.

Implementation details: We keep the same training hyperparameters for all experiments. Cross-entropy loss is used for local model training in all methods. The PDL algorithms (VPDL and CYCLE) use Kullback-Leibler (KL) divergence based on predictions as the distillation loss. The optimizer is stochastic gradient descent (SGD) with momentum. The learning rate is initially set to 0.1 and is updated every 25 rounds using a scheduler with a learning rate decay of 0.1. For FL algorithms, we set the number of collaborating rounds to $t_{max} = 100$ and the local update epoch to 1. For the decentralized algorithms, we use 25 epochs of local training before collaboration, followed by 75 rounds of collaboration. The batch size is set to 128 for CIFAR-10 and CIFAR-100, and 32 for Fed-ISIC2019 dataset. Furthermore, $\alpha = 0.5, \lambda_0 = 50, \tau_{opt} = 0.25$ and $\tau_{max} = 0.75$. We conduct our experiments on NVIDIA A100-PCIE-40GB GPUs on an internal cluster server, with each run utilizing a single GPU. The execution time for each run averages around 1.35 hours.

Evaluation metrics: We assess the accuracy of the trained models based on their mean validation accuracy (MVA) and mean collaboration gain (MCG) across all participants. To evaluate collaborative fairness, we use the collaboration gain spread (CGS). The reputation scores are reported in a matrix form to determine the relative contribution of each client.

5.2 Experimental Results

We start with benchmarking existing algorithms on the CIFAR-10 dataset. Table 1 summarizes the results for different splitting strategies involving $N = 5$ participants. Our key findings are: (i) We assess the performance of three algorithms - FedAvg, VPDL, and CYCLE - using the ResNet18 architecture. These results are shown in Figure 2 and the upper section of Table 1 (rows 3-5). FedAvg has better MCG compared to other methods due to its centralized FL approach, which involves aggregating and sharing full model parameters, resulting in good overall utility. However, when it comes to collaborative fairness, FedAvg falls short of being fair to participants who contribute a larger amount of data. In particular, the CYCLE approach exhibits significantly lower CGS values compared to the FedAvg algorithm in the imbalanced settings. Additionally, our method consistently provides positive collaboration gain to all participants across varied settings. This is not the case for FedAvg or VPDL, which is evident in the outcomes for \mathcal{P}_1 in the imbalanced (0.8, 1) and (0.6, 1) settings. (ii) For comparison with other fairness-aware FL algorithms, we utilize a custom CNN architecture

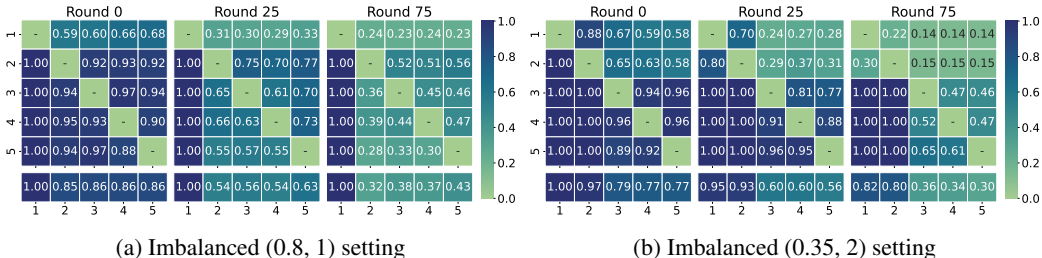


Figure 4: Heatmap visualization of reputation scores for imbalanced settings when $N = 5$.

Table 2: Collaboration gain and spread (MCG, CGS) on CIFAR-10 and CIFAR-100 datasets and the given partition strategies for $N = \{5, 10\}$ using our proposed algorithm.

Dataset		CIFAR-10						CIFAR-100					
N		5			10			5			10		
Split	Method	MVA	MCG	CGS	MVA	MCG	CGS	MVA	MCG	CGS	MVA	MCG	CGS
Homogeneous	VPDL	84.98	1.58	0.71	71.01	1.92	1.58	56.74	7.58	1.20	40.87	10.42	2.48
	CYCLE	86.24	2.84	0.37	73.66	4.57	0.71	57.56	8.40	0.69	41.17	10.72	1.15
Dirichlet (0.5)	VPDL	74.27	6.91	2.31	50.64	1.24	2.24	46.36	10.51	2.59	27.70	3.41	2.80
	CYCLE	76.93	9.57	2.13	53.82	4.42	1.98	47.98	12.13	0.68	28.47	4.18	1.07
Dirichlet (2.0)	VPDL	81.26	3.38	3.72	69.36	5.51	5.00	56.31	12.43	2.31	39.34	9.71	3.16
	CYCLE	83.13	5.25	2.42	72.33	8.48	4.83	57.61	13.73	2.14	39.93	10.30	1.97
Dirichlet (5.0)	VPDL	83.32	2.39	1.94	72.37	4.54	3.96	58.18	9.80	1.38	41.86	10.03	2.92
	CYCLE	84.80	3.86	1.15	74.83	7.00	3.72	59.67	11.29	1.08	41.92	10.09	1.38

used in [28]. This is necessary because CGSV works better on simpler architectures. The results are shown in Figure 3 and the bottom part of Table 1 (rows 6-9). Our method has better or comparable CG values when compared to CFFL, RFFL, and CGSV in most of the scenarios. In terms of fairness, we surpass other approaches by achieving the lowest CGS values in all but one scenario: imbalanced (0.8, 1) setting, where it is on par with RFFL. Notably, CYCLE consistently achieves positive gains for all participants, whereas other methods degrade performance for the most contributing participant (see Fig. 3). Next, we assess the performance of our approach on the CIFAR-10 and CIFAR-100 datasets with different number of participants ($N \in \{5, 10\}$) and data splitting scenarios (Tab. 2). In all the settings, we consistently achieve positive collaboration gain for all participants and the CYCLE method consistently has lower CGS compared to VPDL, indicating the effectiveness of our method.

Reputation scoring visualization: Fig. 4 visualizes the computed reputation scores in three collaboration rounds: $t = 0, 25, 75$ using heatmap plots. In Fig 4a, where participants have imbalanced data (with \mathcal{P}_1 having 80% of the data), our method can already identify distinct patterns of each participant’s data value from the beginning of the collaboration. The heatmap figure emphasizes that the higher is importance given to \mathcal{P}_1 by all the other participants. As the collaboration progresses, the reputation of \mathcal{P}_1 intensifies further, while the reputation scores of other participants decrease. Towards the end of the collaboration, the values converge to a state where participants with an equal amount of data receive equal reputation scores. A similar pattern can be observed in Fig 4b, where the first two participants possess larger amounts of data. While the first five rows of the heatmap figures depict the raw reputation scores calculated using Eq. 5, the sixth row at the bottom represents the average reputation scores aggregated over all the rounds.

Free Rider Study: In this study involving $N = 5$ participants with homogeneous data splitting scenario, we simulate varying degrees of label flipping at participant \mathcal{P}_5 . We tested the label flipping rates of 0.2, 0.5 and 1.0. From Fig. 5, it is evident that the honest participants (participants $\mathcal{P}_1, \dots, \mathcal{P}_4$) quickly discern the anomaly with \mathcal{P}_5 , detecting it as a potential threat. Consequently, they assign a reputation score of 0.0 to \mathcal{P}_5 , indicating a cessation of updates to this participant. On the other hand, \mathcal{P}_5 accurately recognized that the other participants were beneficial when the label flipping rate was at 0.2, but this positive assessment drops to zero for the case when the label space of \mathcal{P}_5 become completely different.

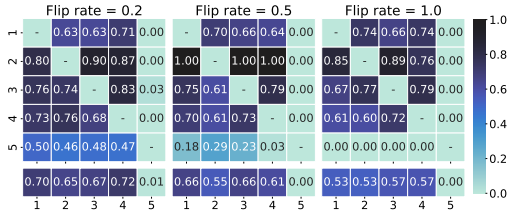


Figure 5: Heatmap visualization of reputation scores when the labels at one of the participants \mathcal{P}_5 get corrupted by label flipping. When the flip rate is large, the “malicious” client is quickly identified by the other participants and it gets shunted out of the collaboration.

6 Conclusion

This paper proposes a novel reputation-based adaptive sharing algorithm, specifically tailored for decentralized learning scenarios. Through theoretical and empirical analyses, this work has illustrated the algorithm’s superior capabilities in achieving collaborative fairness. In future, we will theoretically study the convergence characteristics of the proposed protocol.

References

- [1] Anish Athalye, Nicholas Carlini, and David Wagner. Obfuscated gradients give a false sense of security: Circumventing defenses to adversarial examples. In *International conference on machine learning*, pages 274–283. PMLR, 2018.
- [2] Eugene Bagdasaryan, Andreas Veit, Yiqing Hua, Deborah Estrin, and Vitaly Shmatikov. How to backdoor federated learning. In *International Conference on Artificial Intelligence and Statistics*, pages 2938–2948. PMLR, 2020.
- [3] Centers for Medicare & Medicaid Services. The Health Insurance Portability and Accountability Act of 1996 (HIPAA). Online at <http://www.cms.hhs.gov/hipaa/>, 1996.
- [4] Hongyan Chang, Virat Shejwalkar, Reza Shokri, and Amir Houmansadr. Cronus: Robust and heterogeneous collaborative learning with black-box knowledge transfer. *arXiv preprint arXiv:1912.11279*, 2019.
- [5] Yae Jee Cho, Divyansh Jhunjhunwala, Tian Li, Virginia Smith, and Gauri Joshi. Maximizing global model appeal in federated learning. *arXiv preprint arXiv:2205.14840*, 2022.
- [6] Yae Jee Cho, Divyansh Jhunjhunwala, Tian Li, Virginia Smith, and Gauri Joshi. To federate or not to federate: incentivizing client participation in federated learning. In *Workshop on Federated Learning: Recent Advances and New Challenges (in Conjunction with NeurIPS 2022)*, 2022.
- [7] Christopher A. Choquette-Choo, Natalie Dullerud, Adam Dziedzic, Yunxiang Zhang, Somesh Jha, Nicolas Papernot, and Xiao Wang. CaPC Learning: Confidential and Private Collaborative Learning. In *International Conference on Learning Representations*, 2021.
- [8] Cynthia Dwork, Aaron Roth, et al. The algorithmic foundations of differential privacy. *Foundations and Trends® in Theoretical Computer Science*, 9(3–4):211–407, 2014.
- [9] Úlfar Erlingsson, Vitaly Feldman, Ilya Mironov, Ananth Raghunathan, Shuang Song, Kunal Talwar, and Abhradeep Thakurta. Encode, shuffle, analyze privacy revisited: Formalizations and empirical evaluation. *arXiv preprint arXiv:2001.03618*, 2020.
- [10] European Parliament and Council of the European Union. Regulation (EU) 2016/679 of the European Parliament and of the Council, The General Data Protection Regulation ("GDPR"), 2016.
- [11] Jianping Gou, Baosheng Yu, Stephen J Maybank, and Dacheng Tao. Knowledge distillation: A survey. *International Journal of Computer Vision*, 129:1789–1819, 2021.
- [12] Ruoxi Jia, David Dao, Boxin Wang, Frances Ann Hubis, Nick Hynes, Nezihe Merve Gürel, Bo Li, Ce Zhang, Dawn Song, and Costas J Spanos. Towards efficient data valuation based on the shapley value. In *The 22nd International Conference on Artificial Intelligence and Statistics*, pages 1167–1176. PMLR, 2019.
- [13] Meirui Jiang, Holger R. Roth, Wenqi Li, Dong Yang, Can Zhao, Vishwesh Nath, Daguang Xu, Qi Dou, and Ziyue Xu. Fair federated medical image segmentation via client contribution estimation. In *Proceedings of the IEEE/CVF Conference on Computer Vision and Pattern Recognition (CVPR)*, pages 16302–16311, June 2023.
- [14] Peter Kairouz, Ziyu Liu, and Thomas Steinke. The distributed discrete gaussian mechanism for federated learning with secure aggregation. In *International Conference on Machine Learning*, pages 5201–5212. PMLR, 2021.
- [15] Alex Krizhevsky, Geoffrey Hinton, et al. Learning multiple layers of features from tiny images. *Toronto, ON, Canada*, 2009.
- [16] Sourav Kumar, A Lakshminarayanan, Ken Chang, Feri Guretno, Ivan Ho Mien, Jayashree Kalpathy-Cramer, Pavitra Krishnaswamy, and Praveer Singh. Towards more efficient data valuation in healthcare federated learning using ensembling. In *Distributed, Collaborative, and Federated Learning, and Affordable AI and Healthcare for Resource Diverse Global Health*:

- Third MICCAI Workshop, DeCaF 2022, and Second MICCAI Workshop, FAIR 2022, Held in Conjunction with MICCAI 2022, Singapore, September 18 and 22, 2022, Proceedings*, pages 119–129. Springer, 2022.
- [17] Balaji Lakshminarayanan, Alexander Pritzel, and Charles Blundell. Simple and scalable predictive uncertainty estimation using deep ensembles. *Advances in neural information processing systems*, 30, 2017.
- [18] Lingjuan Lyu, Xinyi Xu, Qian Wang, and Han Yu. Collaborative fairness in federated learning. *Federated Learning: Privacy and Incentive*, pages 189–204, 2020.
- [19] Brendan McMahan, Eider Moore, Daniel Ramage, Seth Hampson, and Blaise Agueria y Arcas. Communication-efficient learning of deep networks from decentralized data. In *Artificial intelligence and statistics*, pages 1273–1282. PMLR, 2017.
- [20] H. Brendan McMahan, Daniel Ramage, Kunal Talwar, and Li Zhang. Learning differentially private recurrent language models. In *International Conference on Learning Representations*, 2018.
- [21] Jean Ogier du Terrail, Samy-Safwan Ayed, Edwige Cyffers, and etal. Grimberg, Felix. Flamby: Datasets and benchmarks for cross-silo federated learning in realistic healthcare settings. In *Advances in Neural Information Processing Systems*, volume 35, pages 5315–5334. Curran Associates, Inc., 2022.
- [22] Lloyd S Shapley et al. A value for n-person games. *Princeton University Press Princeton*, 1953.
- [23] Zhuan Shi, Lan Zhang, Zhenyu Yao, Lingjuan Lyu, Cen Chen, Li Wang, Junhao Wang, and Xiang-Yang Li. FedFAIM: A model performance-based fair incentive mechanism for federated learning. *IEEE Transactions on Big Data*, 2022.
- [24] Nurbek Tastan, Samar Fares, Toluwani Aremu, Samuel Horváth, and Karthik Nandakumar. Redefining contributions: Shapley-driven federated learning. In Kate Larson, editor, *Proceedings of the Thirty-Third International Joint Conference on Artificial Intelligence, IJCAI-24*, pages 5009–5017. International Joint Conferences on Artificial Intelligence Organization, 8 2024. Main Track.
- [25] Nurbek Tastan and Karthik Nandakumar. CaPriDe Learning: Confidential and private decentralized learning based on encryption-friendly distillation loss. In *Proceedings of the IEEE/CVF Conference on Computer Vision and Pattern Recognition*, 2023.
- [26] Tianhao Wang, Johannes Rausch, Ce Zhang, Ruoxi Jia, and Dawn Song. A principled approach to data valuation for federated learning. *Federated Learning: Privacy and Incentive*, pages 153–167, 2020.
- [27] Xinyi Xu and Lingjuan Lyu. A reputation mechanism is all you need: Collaborative fairness and adversarial robustness in federated learning. In *International Workshop on Federated Learning for User Privacy and Data Confidentiality in Conjunction with ICML 2021 (FL-ICML’21)*, 2021.
- [28] Xinyi Xu, Lingjuan Lyu, Xingjun Ma, Chenglin Miao, Chuan Sheng Foo, and Bryan Kian Hsiang Low. Gradient driven rewards to guarantee fairness in collaborative machine learning. *Advances in Neural Information Processing Systems*, 34:16104–16117, 2021.
- [29] Jingwen Zhang, Yuezhou Wu, and Rong Pan. Incentive mechanism for horizontal federated learning based on reputation and reverse auction. In *Proceedings of the Web Conference 2021*, pages 947–956, 2021.
- [30] Bo Zhao, Konda Reddy Mopuri, and Hakan Bilen. idlg: Improved deep leakage from gradients. *arXiv preprint arXiv:2001.02610*, 2020.
- [31] Zirui Zhou, Lingyang Chu, Changxin Liu, Lanjun Wang, Jian Pei, and Yong Zhang. Towards fair federated learning. In *Proceedings of the 27th ACM SIGKDD Conference on Knowledge Discovery & Data Mining*, pages 4100–4101, 2021.
- [32] Ligeng Zhu, Zhijian Liu, and Song Han. Deep leakage from gradients. *Advances in neural information processing systems*, 32, 2019.

A Mean Estimation under CYCLE Protocol

Standard FL. The vanilla FedAvg algorithm, a standard FL approach, does not ensure an optimal final model for all participants in a federated setting. Consider a simple scenario involving two clients, $N = 2$, each aiming to estimate the mean of their data distribution by minimizing the loss function $f_k(w) = (w - \theta_k)^2$. However, these clients can't compute the true mean directly due to having only N_k samples from their distributions, denoted $e_{k,j} \sim \mathcal{N}(\theta_k, \nu^2)$, $\forall j \in [N_k]$. Consequently, they minimize the empirical loss function $F_k(w) = (w - \hat{\theta}_k)^2 + (\hat{\theta}_k - \theta_k)^2$, where $\hat{\theta}_k = \frac{1}{N_k} \sum_{j=1}^{N_k} e_{k,j}$, leading to $\hat{w}_k = \hat{\theta}_k$ as the minimizer of $F_k(w)$.

Additionally, the following quantities are defined:

$$\gamma^2 := \frac{\nu^2}{N}; \quad \gamma_G^2 = \left(\frac{\theta_1 - \theta_2}{2} \right)^2 \quad (6)$$

Note that the distribution of the empirical means themselves are distributed normally, due to the linear additivity property of independent normal random variables. This setting is similar to [6, 5], albeit with a few modifications.

$$\hat{\theta}_1 \sim \mathcal{N}(\theta_1, \gamma^2); \quad \hat{\theta}_2 \sim \mathcal{N}(\theta_2, \gamma^2) \quad (7)$$

Lemma A.1. (Cho et al. [6]) *The probability (likelihood) that the model obtained from collaborative training outperforms the standalone training model is upper-bounded by $2 \exp\left(-\frac{\gamma_G^2}{5\gamma^2}\right)$ in a standard FL framework.*

Proof. We analyze the probability that the global model obtained using FedAvg algorithm is superior to one trained independently (standalone). The model in the standard FL approach is defined as:

$$w = \frac{\hat{\theta}_1 + \hat{\theta}_2}{2} \quad (8)$$

Then, the **usefulness** of the federated model can be measured in the following way:

$$\begin{aligned} & \mathbb{P}\left((w - \theta_1)^2 \leq (\hat{\theta}_1 - \theta_1)^2\right) \\ &= \mathbb{P}\left(\left(\frac{\hat{\theta}_1 + \hat{\theta}_2}{2} - \theta_1\right)^2 \leq (\hat{\theta}_1 - \theta_1)^2\right) \end{aligned} \quad (9)$$

$$= \mathbb{P}\left(\left(\frac{\hat{\theta}_1 + \hat{\theta}_2}{2} - \theta_1\right)^2 - (\hat{\theta}_1 - \theta_1)^2 \leq 0\right) \quad (10)$$

$$= \mathbb{P}\left(\left(\frac{\hat{\theta}_2 - \hat{\theta}_1}{2}\right)^2 + 2(\hat{\theta}_1 - \theta_1)\left(\frac{\hat{\theta}_2 - \hat{\theta}_1}{2}\right) \leq 0\right) \quad (11)$$

$$\begin{aligned} &= \mathbb{P}\left(\left\{\left(\frac{\hat{\theta}_2 - \hat{\theta}_1}{2}\right)^2 + 2(\hat{\theta}_1 - \theta_1)\left(\frac{\hat{\theta}_2 - \hat{\theta}_1}{2}\right) \leq 0\right\} \cap \{\hat{\theta}_2 > \hat{\theta}_1\}\right) \\ &\quad + \mathbb{P}\left(\left\{\left(\frac{\hat{\theta}_2 - \hat{\theta}_1}{2}\right)^2 + 2(\hat{\theta}_1 - \theta_1)\left(\frac{\hat{\theta}_2 - \hat{\theta}_1}{2}\right) \leq 0\right\} \cap \{\hat{\theta}_2 \leq \hat{\theta}_1\}\right) \end{aligned} \quad (12)$$

$$\begin{aligned} &= \mathbb{P}\left(\left\{\left(\frac{\hat{\theta}_2 - \hat{\theta}_1}{2}\right) + 2(\hat{\theta}_1 - \theta_1) \leq 0\right\} \cap \{\hat{\theta}_2 > \hat{\theta}_1\}\right) \\ &\quad + \mathbb{P}\left(\left\{\left(\frac{\hat{\theta}_2 - \hat{\theta}_1}{2}\right)^2 + 2(\hat{\theta}_1 - \theta_1)\left(\frac{\hat{\theta}_2 - \hat{\theta}_1}{2}\right) \leq 0\right\} \cap \{\hat{\theta}_2 \leq \hat{\theta}_1\}\right) \end{aligned} \quad (13)$$

$$\leq \mathbb{P}\left(\left(\frac{\widehat{\theta}_2 - \widehat{\theta}_1}{2}\right) + 2(\widehat{\theta}_1 - \theta_1) \leq 0\right) + \mathbb{P}(\widehat{\theta}_2 - \widehat{\theta}_1 \leq 0) \quad (14)$$

$$= \mathbb{P}(Z_1 \leq 0) + \mathbb{P}(Z_2 \leq 0) \quad \text{where } Z_1 \sim \mathcal{N}\left(\gamma_G, \frac{5}{2}\gamma^2\right), Z_2 \sim \mathcal{N}(2\gamma_G, 2\gamma^2) \quad (15)$$

$$\leq \exp\left(-\frac{\gamma_G^2}{5\gamma^2}\right) + \exp\left(-\frac{\gamma_G^2}{\gamma^2}\right) \leq 2 \exp\left(-\frac{\gamma_G^2}{5\gamma^2}\right) \quad (16)$$

where (10) uses $\mathbb{P}(A) = \mathbb{P}(A \cap B) + \mathbb{P}(A \cap B^C)$, (14) uses $\mathbb{P}(A \cap B) \leq \mathbb{P}(A)$, (15) uses the linear additivity property of independent normal random variables and (7), (16) uses a Chernoff bound. \square

CYCLE Algorithm. The CYCLE algorithm uniquely incorporates the reputations of each client during the aggregation of their computed means. Considering the scenario from the perspective of Client 1, who possesses an estimate $\widehat{\theta}_1$ and receives $\widehat{\theta}_2$ from Client 2, the aggregation is expressed as:

$$w_1 = \left(1 - \frac{r_{1,2}}{2}\right)\widehat{\theta}_1 + \frac{r_{1,2}}{2}\widehat{\theta}_2 \quad (17)$$

As CYCLE operates on a decentralized principle, each client develops its final model based on individual reputations denoted by r . For example, for Client 2, the model is:

$$w_2 = \left(1 - \frac{r_{2,1}}{2}\right)\widehat{\theta}_2 + \frac{r_{2,1}}{2}\widehat{\theta}_1 \quad (18)$$

Notably, w_1 and w_2 are not necessarily the same due to the distinct reputation scores. The following discussion will simplify the notation by dropping indices and focusing on the aggregation process from the perspective of Client 1.

Reputation Scoring. In the CYCLE algorithm, each participant calculates the reputation of their collaborators by assessing the distance between their shared means, denoted as $d = \left(\frac{\widehat{\theta}_2 - \widehat{\theta}_1}{2}\right)^2$. This distance is then used to determine their reputations as follows:

$$r = \begin{cases} 1.0 & \text{if } d \leq 1 \\ 2 - d & \text{if } 1 < d \leq 2 \\ 0.0 & \text{if } d > 2 \end{cases} \quad (19)$$

Here, d represents the empirical heterogeneity parameter, referred to as $\widehat{\gamma}_G^2$. The rationale for the assigned values is based on the degree of heterogeneity (19):

- If $\widehat{\gamma}_G^2 < 1$, it indicates minimal heterogeneity, suggesting that participants can benefit significantly from collaboration.
- If $\widehat{\gamma}_G^2 > 2$, it signals substantial heterogeneity, advising participants to avoid collaboration.

Thus, the reputation scores are directly influenced by the empirical heterogeneity observed between the participants.

Cost Function. To evaluate the CYCLE algorithm against the standard, centralized FL algorithm, we consider the empirical losses each participant ends up solving. In FedAvg, all clients achieve the common mean:

$$w = \frac{\widehat{\theta}_1 + \widehat{\theta}_2}{2} \quad (20)$$

and the empirical loss for Client 1 is:

$$F_1(w) = F_1\left(\frac{\widehat{\theta}_1 + \widehat{\theta}_2}{2}\right) = \widehat{\gamma}_G^2 + (\widehat{\theta}_1 - \theta_1)^2 \quad (21)$$

This formulation shows that each client encounters non-reducible loss terms in the FedAvg algorithm. For the CYCLE algorithm, the model aggregation is reputation-weighted:

$$w = \left(1 - \frac{r}{2}\right)\widehat{\theta}_1 + \frac{r}{2}\widehat{\theta}_2 \quad (22)$$

yielding the empirical loss:

$$F_1(w) = r^2 \hat{\gamma}_G^2 + (\hat{\theta}_1 - \theta_1)^2 \quad (23)$$

In CYCLe, the empirical heterogeneity parameter $\hat{\gamma}_G^2$ is adjusted using the reputation scores r , allowing each client to potentially achieve a final model that is as good as or better than their standalone model. Conversely, in FedAvg, all clients share the same final model. As the heterogeneity between clients increases (γ_G^2), the efficacy (usefulness) of the global model significantly diminishes, as highlighted in Lemma A.1. This comparison illustrates the advantage of CYCLe in managing heterogeneity among the participants to enhance individual outcomes.

Minimizing the CYCLe Objective: Ensuring Positive Outcomes. Unlike standard FL where increasing true heterogeneity γ_G^2 drastically reduces the usefulness of the global model (as noted in Lemma A.1), CYCLe modulates the aggregation phase using reputation scores which are derived from the empirical heterogeneity parameter $\hat{\gamma}_G^2$ (19).

Theorem A.1. *The probability (likelihood) that the model obtained through collaboration (w) surpasses a standalone-trained model ($\hat{\theta}$) is lower bounded by $\frac{1}{8} \exp\left(-\frac{1}{4\gamma^2}\right)$ in the CYCLe algorithm.*

Proof. We assess the performance (usefulness) of the collaborative model for client i using:

$$\mathbb{P}\left((w_i - \theta_i)^2 \leq (\hat{\theta}_i - \theta_i)^2\right) \quad (24)$$

This analysis includes both of the scenarios: (i) $\hat{\theta}_1 = \hat{\theta}_2$ which directly implies a probability of 1.0, and (ii) a significant difference between $\hat{\theta}_1$ and $\hat{\theta}_2$ ($\hat{\gamma}_G^2 \gg 0$), leading to no collaboration, also resulting in a probability of 1.0. The CYCLe algorithm is not interested in obtaining a final global model and each client is self-interested in minimizing their own objective functions.

Case 1: $\hat{\gamma}_G^2 \leq 1$

$$\mathbb{P}\left((w_1 - \theta_1)^2 \leq (\hat{\theta}_1 - \theta_1)^2\right) \quad (25)$$

$$= \mathbb{P}\left((w_1 - \hat{\theta}_1)^2 + 2(w_1 - \hat{\theta}_1)(\hat{\theta}_1 - \theta_1) \leq 0\right) \quad (26)$$

$$= \mathbb{P}\left(\left(\frac{\hat{\theta}_2 - \hat{\theta}_1}{2}\right)^2 + 2\left(\frac{\hat{\theta}_2 - \hat{\theta}_1}{2}\right)(\hat{\theta}_1 - \theta_1) \leq 0\right) \quad (27)$$

$$= \mathbb{P}\left(\left\{\left(\frac{\hat{\theta}_2 - \hat{\theta}_1}{2}\right)^2 + 2\left(\frac{\hat{\theta}_2 - \hat{\theta}_1}{2}\right)(\hat{\theta}_1 - \theta_1) \leq 0\right\} \cap \{\hat{\theta}_2 > \hat{\theta}_1\}\right) \\ + \mathbb{P}\left(\left\{\left(\frac{\hat{\theta}_2 - \hat{\theta}_1}{2}\right)^2 + 2\left(\frac{\hat{\theta}_2 - \hat{\theta}_1}{2}\right)(\hat{\theta}_1 - \theta_1) \leq 0\right\} \cap \{\hat{\theta}_2 \leq \hat{\theta}_1\}\right) \quad (28)$$

$$\geq \mathbb{P}\left(\{1 + 2(\hat{\theta}_1 - \theta_1) \leq 0\} \cap \{\hat{\theta}_2 > \hat{\theta}_1\}\right) \quad (29)$$

$$= \mathbb{P}\left(\{\hat{\theta}_1 - \theta_1 \leq -\frac{1}{2}\} \cap \{\hat{\theta}_2 > \hat{\theta}_1\}\right) \quad (30)$$

$$= \mathbb{P}(\hat{\theta}_1 < \hat{\theta}_2) \mathbb{P}(\hat{\theta}_1 - \theta_1 \leq -\frac{1}{2} | \hat{\theta}_1 < \hat{\theta}_2) \quad (31)$$

$$\geq \mathbb{P}(\hat{\theta}_1 < \hat{\theta}_2) \mathbb{P}(\hat{\theta}_1 - \theta_1 \leq -\frac{1}{2}) \quad (32)$$

$$= \mathbb{P}(\hat{\theta}_1 < \hat{\theta}_2) \mathbb{P}(Z > \frac{1}{2\gamma}) \quad \text{where } Z \sim \mathcal{N}(0, 1) \quad (33)$$

$$\geq \frac{1}{8} \exp\left(-\frac{1}{4\gamma^2}\right) \quad (34)$$

where (27) uses the reputation score $r = 1$ when $\hat{\gamma}_G^2 < 1$ (refer to (19)), (28) uses $\mathbb{P}(A) = \mathbb{P}(A \cap B) + \mathbb{P}(A \cap B^C)$, (29) uses the definition of $\hat{\gamma}_G^2 \leq 1$ and the second part of expression can

be dropped since $\hat{\gamma}_G$ can take values from -1 to 0 , it can be assigned zero probability, (32) uses $\mathbb{P}(A|B) \geq \mathbb{P}(A)$, (33) uses $\hat{\theta}_1 - \theta_1 \sim \mathcal{N}(0, \gamma^2)$, (34) $\mathbb{P}(\hat{\theta}_1 < \hat{\theta}_2) \geq \frac{1}{2}$ and $\mathbb{P}(Z \geq x) \geq \frac{1}{4} \exp(-x^2)$ where $Z \sim \mathcal{N}(0, 1)$. The similar bound can be found for the second client.

Case 2: $1 < \hat{\gamma}_G^2 \leq 2$

In this case, we can follow the similar approach above and we get:

$$\mathbb{P}\left((w_1 - \theta_1)^2 \leq (\hat{\theta}_1 - \theta_1)^2\right) \quad (35)$$

$$= \mathbb{P}\left((w_1 - \hat{\theta}_1)^2 + 2(w_1 - \hat{\theta}_1)(\hat{\theta}_1 - \theta_1) \leq 0\right) \quad (36)$$

$$= \mathbb{P}\left(\left(\frac{r}{2}(\hat{\theta}_2 - \hat{\theta}_1)\right)^2 + r(\hat{\theta}_2 - \hat{\theta}_1)(\hat{\theta}_1 - \theta_1) \leq 0\right) \quad (37)$$

$$= \mathbb{P}\left(r\left(\frac{\hat{\theta}_2 - \hat{\theta}_1}{2}\right)^2 + 2\left(\frac{\hat{\theta}_2 - \hat{\theta}_1}{2}\right)(\hat{\theta}_1 - \theta_1) \leq 0\right) \quad (38)$$

$$\geq \mathbb{P}\left(\{1 + 2(\hat{\theta}_1 - \theta_1) \leq 0\} \cap \{\hat{\theta}_2 > \hat{\theta}_1\}\right) \quad (39)$$

$$\geq \frac{1}{8} \exp\left(-\frac{1}{4\gamma^2}\right) \quad (40)$$

The reason behind getting the same bound as in Case 1 is that the expression in (38) is maximized when $r = (2 - \hat{\gamma}_G^2) = 1$, which necessitates $\hat{\gamma}_G \approx 1$, when $\hat{\theta}_1 < \hat{\theta}_2$.

Case 3: $\hat{\gamma}_G^2 > 2$

$$\mathbb{P}\left((w_1 - \theta_1)^2 \leq (\hat{\theta}_1 - \theta_1)^2\right) = \left((\hat{\theta}_1 - \theta_1)^2 \leq (\hat{\theta}_1 - \theta_1)^2\right) = 1 \quad (41)$$

where $w_1 = \left(1 - \frac{r}{2}\right)\hat{\theta}_1 + \frac{r}{2}\hat{\theta}_2 = \hat{\theta}_1$, since $r = 0$ for $\hat{\gamma}_G^2 > 2$ (Eqs. 22, 19).

As such, CYCLE effectively adapts to various degrees of heterogeneity, ensuring that collaboration invariably enhances or matches the standalone training performance. This is quantitatively supported by a lower bound of $\frac{1}{8} \exp\left(-\frac{1}{4\gamma^2}\right)$, demonstrating robustness against heterogeneity effects. □

B Numerical Experiments

B.1 Varying Degrees of Heterogeneity

For the first experiment, we adopt the scenario outlined in previous studies [6, 5]. For the simulation involving two clients, we define the true means of the clients as $\theta_1 = 0, \theta_2 = \gamma_G$ where $\gamma_G \in [0, 5]$. The empirical means, $\hat{\theta}_1$ and $\hat{\theta}_2$, are sampled from the distribution $\mathcal{N}(\theta_1, 1)$ and $\mathcal{N}(\theta_2, 1)$ respectively, with equal sample sizes ($N_1 = N_2 = N$). The average usefulness is calculated over 10000 runs.

The results, depicted in Figure 6, highlight the differing impacts of heterogeneity on the final model's usefulness. Under the FedAvg protocol, as heterogeneity increases, the global model's usefulness drops drastically, potentially disadvantaging each client by diverging from their optimal solutions (empirical means). Conversely, the CYCLE approach exhibits an increase in the usefulness of the resultant models (w_i) irrespective of the heterogeneity level. This indicates an effective mechanism within CYCLE for clients to discern and select good collaborators based on the proximity of their updates. In scenarios of pronounced heterogeneity, resulting in low reputation scores, clients are incentivized to rely more heavily on their own updates, effectively mitigating collaboration when it proves detrimental.

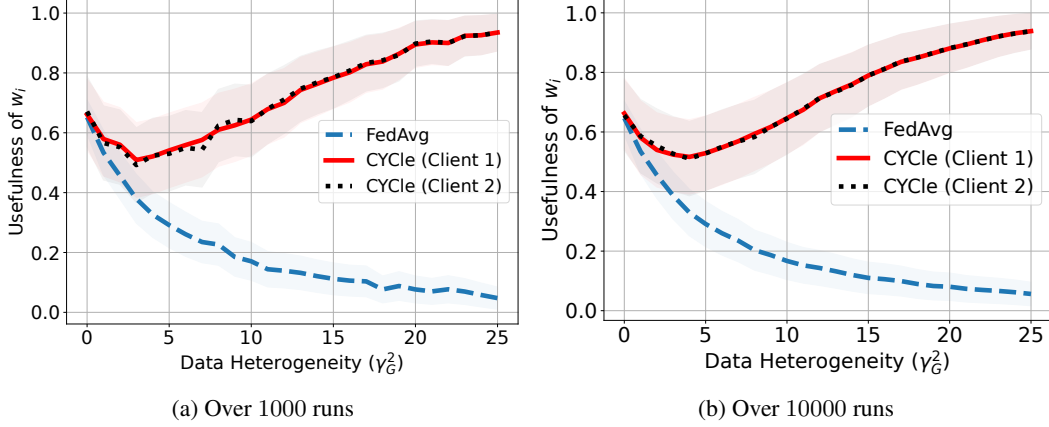


Figure 6: Numerical study on the usefulness of the model obtained after collaboration ($\mathbb{P}((w_i - \theta_i)^2 \leq (\hat{\theta}_i - \theta_i)^2)$) in two client mean estimation. In FedAvg, a single global model is used, whereas in CYCLE, each client computes their model (w_i) independently.

B.2 Imbalanced Data

In this experiment, we consider a scenario where both clients share the same true mean $\theta_1 = \theta_2 = 0$, effectively setting the true heterogeneity parameter $\gamma_G^2 = 0$. Despite this, the clients differ in their number of samples, influencing their empirical means. Specifically, $\hat{\theta}_1$ and $\hat{\theta}_2$ are drawn from distributions $\mathcal{N}(0, \frac{\sigma^2}{N_1})$ and $\mathcal{N}(0, \frac{\sigma^2}{N_2})$, respectively, with σ^2 set to 5.

The results, presented in Figure 7, illustrate the differential impacts of collaboration based on sample size. Collaboration tends to benefit Client 2 more than Client 1, with Client 1 being the higher-contributing client in terms of data. The variance of Client 1 decreases as their data ratio increases, suggesting that Client 1 would benefit from limiting trust in Client 2’s contributions under significant data imbalances. In contrast, the variance for Client 2 remains relatively the same regardless of the data ratio.

Figure 7 (right side) demonstrates the varying utilities of collaboration for each client. For Client 1, the usefulness of collaboration decreases as the data ratio becomes more skewed, whereas it remains constant for Client 2, implying that the collaboration is useful for Client 2. Notably, the FedAvg approach generally results in worse outcomes compared to both clients in the CYCLE scenario, especially as imbalances in data contribution increase.

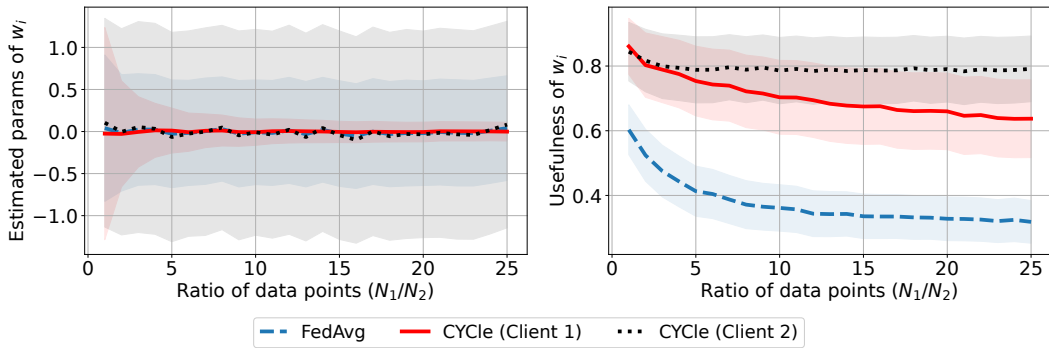


Figure 7: Numerical study on the impact of data imbalance on model usefulness ($\mathbb{P}((w_i - \theta_i)^2 \leq (\hat{\theta}_i - \theta_i)^2)$) and the depiction of θ_i, σ_i estimates for $w_i \sim \mathcal{N}(\theta_i, \sigma_i^2)$ in two client mean estimation across varying degrees of data ratios.

C Additional Results

This section is organized in the following manner:

1. Heatmap visualizations of reputation scores for the remaining data splitting scenarios, which include homogeneous, Dirichlet (0.5), and imbalanced (0.6, 1) cases.
2. Remaining results of Table 2.
3. Details of the Fed-ISIC2019 data distribution and heatmap visualization of reputation scores for Fed-ISIC2019.
4. Experimental results on the CIFAR-100 dataset.
5. More analysis of the imbalanced data splitting scenario.
6. More analysis of the free rider scenario.
7. Trade-off between MCG and CGS.
8. Hyperparameter sensitivity.

C.1 Reputation Score Visualization

In Figure 8, we present the reputation scores calculated on the CIFAR-10 dataset for a group of five participants ($N = 5$). The figure illustrates the results at rounds $t = 0, 25, 75$, under different data partitioning schemes: (i) homogeneous, (ii) heterogeneous (Dirichlet ($\delta = 0.5$)), (iii) imbalanced ($\kappa = 0.6, m = 1$). In the homogeneous setting, participants have similar reputation scores that correlate with the sizes of the datasets they hold. Over time, these scores trend downwards as the cross-entropy loss gains prominence over the total distillation loss (Eq. 1). The heterogeneous and imbalanced (0.6, 1) scenarios exhibit a similar pattern, where the reputation scores align with the size of the data they possess. In the latter scenario, since \mathcal{P}_1 holds 60% of the data, its reputation remains consistent, prompting other participants to engage more actively in collaboration to receive updates from this major contributor.

It must be noted that even when dataset sizes are identical among participants, as seen in homogeneous (\mathcal{P}_1 to \mathcal{P}_5) and imbalanced (0.6, 1) (\mathcal{P}_2 to \mathcal{P}_5) data splitting scenarios, there may be stochastic variations in data quality resulting in higher reputation scores for some participants compared to others. For instance, in Fig. 8c, \mathcal{P}_3 is assigned a marginally higher reputation score by the other participants, despite having an identical dataset size as $\mathcal{P}_2, \mathcal{P}_4$, and \mathcal{P}_5 .

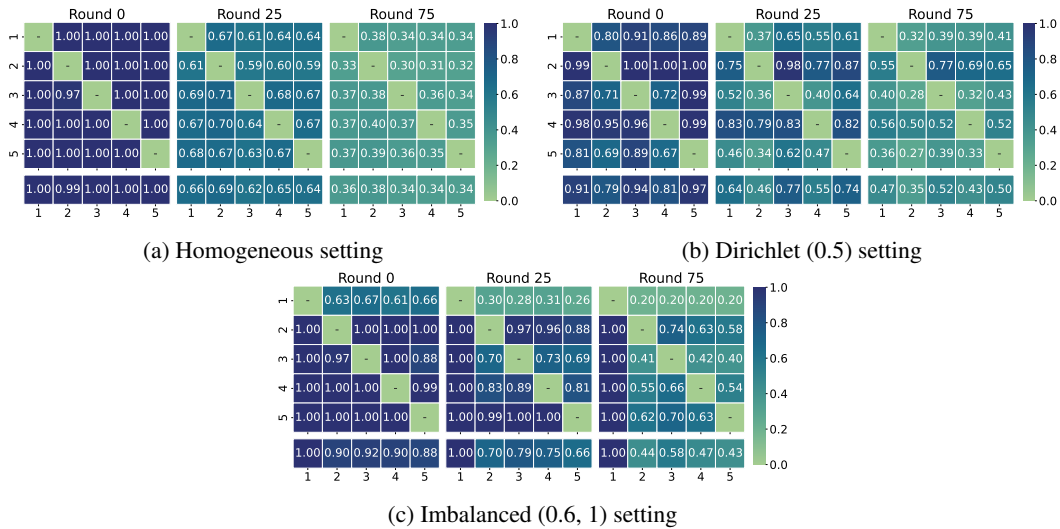


Figure 8: Heatmap visualization of reputation scores for the given number of participants $N = 5$ and data partitioning schemes: (a) Homogeneous, (b) Dirichlet (0.5) and (c) Imbalanced (0.6, 1).

Table 3: Collaboration gain and spread (MCG, CGS) on CIFAR-10 and CIFAR-100 datasets and the given partition strategies for $N = 2$ using our proposed algorithm. This table supplements Table 2, which covers $N = \{5, 10\}$.

Split	Method	CIFAR-10			CIFAR-100		
		MVA	MCG	CGS	MVA	MCG	CGS
Homogeneous	VPDL	91.99	0.41	0.08	71.52	4.87	0.55
	CYCLe	92.58	1.00	0.01	72.03	5.38	0.22
Dirichlet (0.5)	VPDL	84.90	1.45	1.88	64.99	8.95	0.31
	CYCLe	88.82	5.37	0.76	66.37	10.33	0.25
Dirichlet (2.0)	VPDL	89.93	0.09	0.22	70.57	5.52	0.66
	CYCLe	91.00	1.16	0.15	72.09	7.04	0.18
Dirichlet (5.0)	VPDL	90.36	0.24	0.08	71.45	4.95	0.89
	CYCLe	91.29	1.17	0.03	72.12	5.62	0.36

C.2 Remaining Results of Table 2

This section presents the continuation of our analysis on the collaboration gain and spread (MCG, CGS) for CIFAR-10 and CIFAR-100 datasets using our proposed algorithm. Table 2 provided data for scenarios with $N \in \{5, 10\}$ participants. In this continuation, as detailed in Table 3, we include the results of the scenario when $N = 2$.

C.3 Fed-ISIC2019 experiments

Fed-ISIC2019: We evaluate our framework on the real-world non-IID Fed-ISIC2019 dataset. Note that for easy visualization, the participants in this experiment are sorted in the decreasing order of their dataset size. Fig. 9a displays the computed reputation scores for the collaboration rounds $t = 0, 25, 75$. We observe that our framework captures distribution shift, as evidenced by the fact that the data held by the first client does not overlap with that of other clients (as shown in UMAP visualization in Figure 1f of [21]).

Data Distribution. Figure 9b displays a heatmap plot illustrating the distribution of data by class among participants. In Figure 9a, it is evident that despite \mathcal{P}_1 having the bulk of the data, it has a noticeable distribution shift compared to other participants. This indicates that other participants are not allocated certain classes due to the specific distribution settings employed in [21]. It is noteworthy that initially, \mathcal{P}_1 assigns a lower reputation score to \mathcal{P}_4 . However, over time, \mathcal{P}_4 's reputation improves, a change attributable to the exclusive knowledge of class 8 shared only by \mathcal{P}_1 and \mathcal{P}_4 .

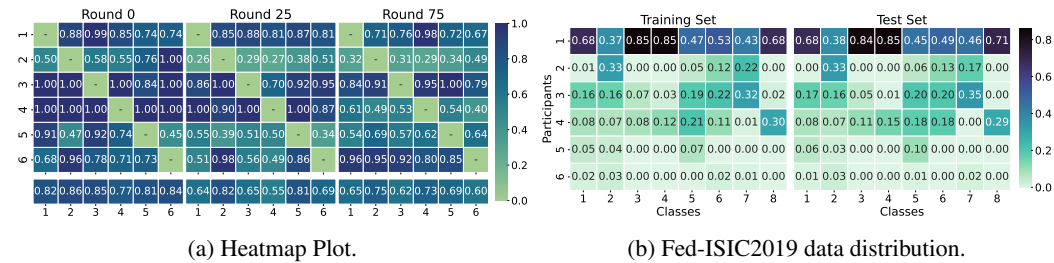


Figure 9: (a) Heatmap visualization of reputation scores for the Fed-ISIC2019 dataset. For easy visualization, the participants in this experiment are sorted in the decreasing order of their dataset size. (b) Fed-ISIC2019 data distribution among participants.

C.4 Experiments on CIFAR-100

We perform the same experiment outlined in Table 1 and Figure 2 on CIFAR-100 dataset. Figure 10 and Table 6 depicts the performance of each participant within the $N = 5$ group across the various data partitioning strategies detailed in Section 5.1. Similar to the observations in Figure 2, in the imbalanced (0.8, 1) scenario, the FedAvg algorithm results in a decline in accuracy for \mathcal{P}_1 , indicative of a negative collaboration gain. Following this, we compile the mean validation accuracy (MVA),

Table 4: Performance comparison on CIFAR-100 dataset: Validation accuracy evaluated with $N = 5$ participants. The table presents the performance of our proposed framework compared to the FedAvg algorithm. We employ MVA (\uparrow), MCG (\uparrow) and CGS (\downarrow) as evaluation metrics.

Setting	Homogeneous			Dirichlet (0.5)			Imbalanced (0.8, 1)			Imbalanced (0.35, 2)			Imbalanced (0.6, 1)		
Metric	MVA	MCG	CGS	MVA	MCG	CGS	MVA	MCG	CGS	MVA	MCG	CGS	MVA	MCG	CGS
FedAvg	70.02	20.86	1.07	68.31	32.46	3.98	72.60	40.77	21.77	70.33	28.22	15.06	70.80	33.56	15.54
VPDL	56.74	7.58	1.20	46.36	10.51	2.59	36.81	4.98	4.84	48.48	6.37	5.19	44.61	7.37	4.98
CYCLE	57.56	8.40	0.69	47.98	12.13	0.68	39.09	7.26	3.30	51.03	8.92	2.40	45.68	8.44	3.00

mean collaboration gain (MCG), and collaboration gain spread (CGS) for each method and data splitting scenario in Table 4.

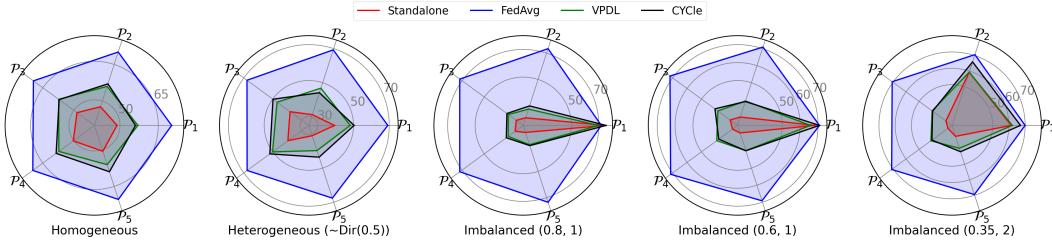


Figure 10: Per-participant performance comparison on CIFAR-100 dataset: Validation accuracy evaluated with $N = 5$ participants.

Table 5: Performance comparison on CIFAR-10 dataset under imbalanced data: Validation accuracy evaluated with $N = 5$ participants. We employ MVA (\uparrow), MCG (\uparrow) and CGS (\downarrow) as evaluation metrics.

Setting	Imbalanced (0.4, 1)			Imbalanced (0.12, 1)			Imbalanced (0.41, 2)			Imbalanced (0.23, 2)			Imbalanced (0.14, 2)		
Metric	MVA	MCG	CGS	MVA	MCG	CGS	MVA	MCG	CGS	MVA	MCG	CGS	MVA	MCG	CGS
FedAvg	91.04	10.38	4.93	90.98	8.02	4.00	90.17	17.48	13.99	91.23	7.73	1.96	90.89	8.42	4.94
VPDL	83.36	2.69	3.04	86.18	3.22	2.74	74.90	2.22	4.17	85.82	2.33	2.09	86.18	3.70	3.67
CYCLE	85.02	4.35	2.26	86.78	3.82	2.41	76.71	4.02	2.27	86.48	2.98	1.17	86.92	4.44	3.47

C.5 Imbalanced Data Study

In this study, we explore a range of values for the parameters κ and m in imbalanced settings, as detailed in Section 5.1. The purpose of this variation is to demonstrate the effectiveness of our proposed CYCLE method in ensuring positive collaboration gains for each participant, showcasing a higher degree of fairness in comparison to FedAvg and VPDL. For a comprehensive view of these results, please see Figure 11 and Table 5.

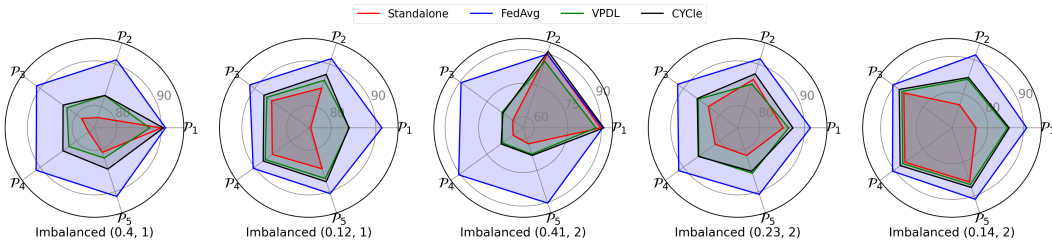


Figure 11: Per-participant performance comparison on CIFAR-10 dataset using the given imbalanced splitting scenarios.

Table 6: Per-participant performance comparison on CIFAR-100 dataset: Validation accuracy evaluated with $N = 5$ participants.

Partition	Number	SA	FedAvg	VPDL	CYCLE	Partition	Number	SA	FedAvg	VPDL	CYCLE
Homogeneous	1	48.85	70.25	57.05	56.10	Imbalanced (0.8, 1)	1	74.50	71.80	70.05	75.30
	2	47.65	70.10	56.00	57.05		2	20.80	73.45	27.40	29.85
	3	48.45	69.55	57.30	57.10		3	21.25	72.10	28.40	29.70
	4	50.25	69.85	57.25	58.55		4	22.25	72.10	28.50	30.20
	5	50.60	70.35	56.10	59.00		5	20.35	73.55	29.70	30.40
Dirichlet (0.5)	1	39.40	69.20	48.15	50.35	Imbalanced (0.35, 2)	1	61.45	70.00	62.10	67.15
	2	31.30	69.25	46.80	44.15		2	59.30	70.60	59.35	65.95
	3	38.00	67.80	47.00	49.80		3	29.65	70.55	40.15	39.80
	4	39.50	67.70	50.10	52.00		4	28.10	70.95	41.05	40.30
	5	31.05	67.60	39.75	43.60		5	32.05	69.55	39.75	41.95

Partition	Number	SA	FedAvg	VPDL	CYCLE
Imbalanced (0.6, 1)	1	68.25	70.80	65.80	70.80
	2	29.90	70.90	39.30	39.00
	3	30.15	71.80	38.70	40.70
	4	28.50	71.35	39.45	38.05
	5	29.40	69.15	39.80	39.85

Table 7: Validation accuracies of participants ($\mathcal{P}_1, \dots, \mathcal{P}_5$) with \mathcal{P}_5 having varying rates of label flipping. The last column refers to the average accuracy of honest participants ($\mathcal{P}_1, \dots, \mathcal{P}_4$). The corresponding figure with reputation scores: Fig. 5.

Setting	\mathcal{P}_1	\mathcal{P}_2	\mathcal{P}_3	\mathcal{P}_4	\mathcal{P}_5	avg
Standalone (\mathcal{B}_n)	83.42	83.67	83.15	83.13	83.63	83.34
Flip rate = 0.0	86.12	87.03	86.33	85.62	86.10	86.28
Flip rate = 0.2	84.95	84.5	84.5	86.45	60.95	85.10
Flip rate = 0.5	84.25	84.65	84.65	83.25	55.80	84.20
Flip rate = 1.0	83.9	84.5	83.95	85.1	10.75	84.36

C.6 Free Rider Study

Table 7, aligned with the scenario depicted in Figure 5, details the values of \mathcal{B}_n and \mathcal{A}_n . It reveals that, in the presence of flipped labels, the collaboration gain declines, reflecting a loss from a participant that holds 20% of the data.

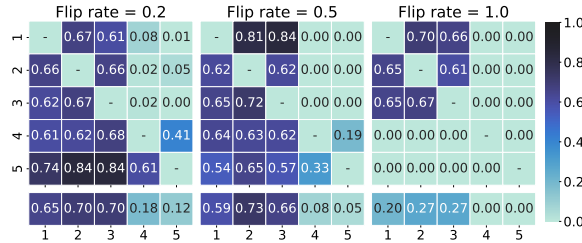


Figure 12: Heatmap visualization of reputation scores when the labels at \mathcal{P}_4 and \mathcal{P}_5 get corrupted by label flipping.

In Figure 12 and Table 8, we examine the outcomes using our CYCLE approach under the varying degrees of label flipping (ranging from 0.0 to 1.0) when two participants (\mathcal{P}_4 and \mathcal{P}_5) are free riders. The findings show that the honest participants ($\mathcal{P}_1, \mathcal{P}_2$, and \mathcal{P}_3) maintain positive collaboration gains, despite the presence of malicious users / free riders. It's observed that when the flip rate is greater than 0, the collaboration gain decreases relative to scenarios where the flip rate is 0. This decline is linked to the fact that these three participants collectively hold only 60% of the total dataset. In this experiment, we use CIFAR-10 dataset and a homogeneous data splitting approach, with other parameters remaining consistent with those detailed in Section 5.1.

C.7 Trade-off between MCG and CGS

Figure 13 presents a plot depicting the MCG and CGS values for 10 different data-split scenarios, which are specified in Table 1 and Table 5. It must be emphasized that the outcomes of our CYCLE approach fall predominantly towards the bottom-right corner of the plot, indicating higher MCG and

Table 8: Validation accuracies of participants ($\mathcal{P}_1, \dots, \mathcal{P}_5$) with \mathcal{P}_4 and \mathcal{P}_5 having varying rates of label flipping. The last column refers to the average accuracy of honest participants ($\mathcal{P}_1, \dots, \mathcal{P}_3$).

Setting	\mathcal{P}_1	\mathcal{P}_2	\mathcal{P}_3	\mathcal{P}_4	\mathcal{P}_5	avg
Standalone (\mathcal{B}_n)	83.42	83.67	83.15	83.13	83.63	83.41
Flip rate = 0.0	86.12	87.03	86.33	85.62	86.10	86.49
Flip rate = 0.2	84.25	84.20	84.10	63.10	65.40	84.18
Flip rate = 0.5	84.30	84.00	83.95	38.95	35.75	84.08
Flip rate = 1.0	84.15	84.20	83.45	3.40	3.10	83.93

lower CGS values. On average, CYCLE achieves the highest MCG and lowest CGS across the 10 scenarios. While competing methods (CFFL, RFFL, and CGSV) may slightly perform better than CYCLE in one metric, they perform significantly worse in the other.

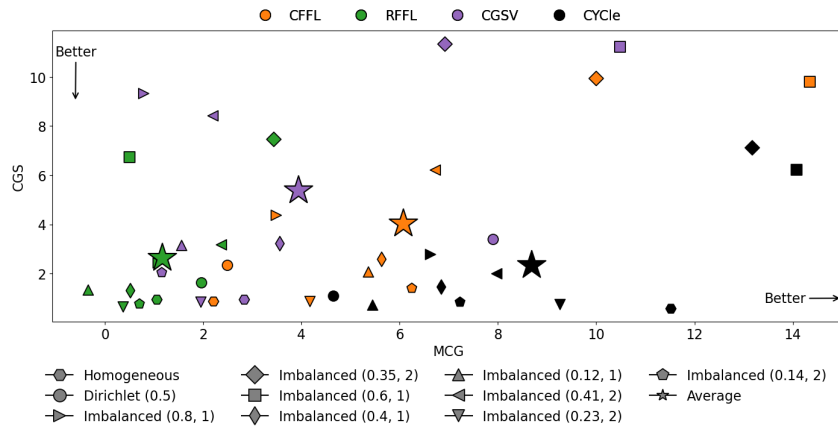


Figure 13: Plot of MCG and CGS values for 10 distinct data splits, ranging from homogeneous to a spectrum of imbalanced scenarios.

C.8 Hyperparameter Sensitivity

We have defined only two hyperparameters in our model, τ_{opt} and τ_{max} , which have a geometric interpretation (degree of gradient alignment required for beneficial collaboration). In our experiments, we set $\tau_{opt} = 0.25$ and $\tau_{max} = 0.75$. Figure 14a shows the sensitivity analysis for these hyperparameters, where it is evident that increasing the values of τ_{max} and τ_{opt} correlates with improved MCG in a homogeneous setting. This is expected as higher values of these parameters bring our algorithm closer to the VPDL framework. However, the MCG and CGS (Figure 14b) values for different hyperparameter settings are comparable, indicating that the reported results are robust.

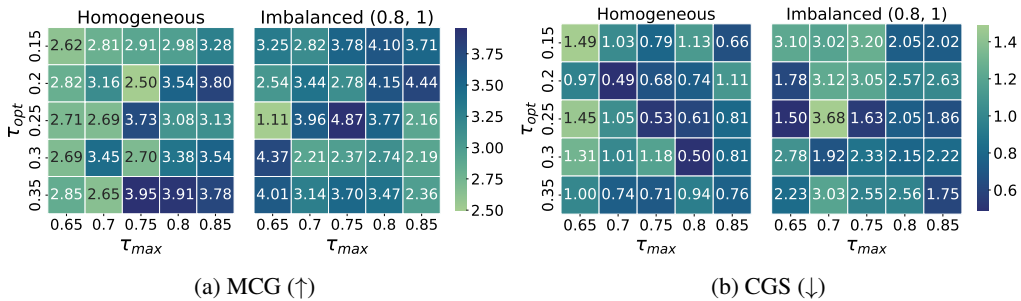


Figure 14: Sensitivity analysis to τ_{opt} and τ_{max} parameters.

C.9 Additional Results

The accuracy metrics for the individual participants for the experiments on CIFAR-10 dataset (corresponding to Figures 2 and 3) are summarized in Table 9 for greater clarity. These results clearly demonstrate the negative gain experienced by participant \mathcal{P}_1 in the imbalanced settings under most existing FL algorithms and how the proposed CYCLE approach overcomes this problem.

Table 9: Per-participant performance comparison on CIFAR-10 dataset: Validation accuracy evaluated with $N = 5$ participants. The left table presents the performance of our proposed framework compared to the FedAvg algorithm. The right table compares collaboration gain and fairness of our proposed CYCLE algorithm with existing works (columns 4-6). We employ MVA (\uparrow), MCG (\uparrow) and CGS (\downarrow) as evaluation metrics.

Partition	No./Metric	SA	FedAvg	VPDL	CYCLE	Partition	No./Metric	SA	CFFL	RFFL	CGSV	CYCLE
Homogeneous	1	83.42	91.02	85.82	86.12	Homogeneous	1	60.98	62.05	61.65	63.32	72.42
	2	83.67	90.32	84.02	87.03		2	59.87	63.60	62.32	63.67	70.88
	3	83.15	90.63	84.70	86.33		3	59.20	61.58	61.07	63.08	71.48
	4	83.13	90.82	85.27	85.62		4	60.50	62.50	60.80	61.88	72.55
	5	83.63	90.23	85.12	86.10		5	61.67	63.53	61.65	64.42	72.43
	MVA	83.40	90.60	84.98	86.24		MVA	60.44	62.65	61.50	63.27	71.95
MCG	0.00	7.20	1.58	2.84	MCG	0.00	2.21	1.05	2.83	11.51		
CGS	0.00	0.48	0.71	0.37	CGS	0.00	0.87	0.95	0.94	0.58		
Dirichlet(0.5)	1	68.47	88.92	74.47	79.48	Dirichlet(0.5)	1	48.17	47.65	48.45	55.30	51.78
	2	65.25	88.48	74.17	73.55		2	48.72	49.28	50.07	53.10	53.20
	3	73.92	88.35	77.17	79.87		3	49.15	51.15	50.70	53.60	53.82
	4	67.55	88.68	74.17	78.70		4	44.17	49.30	45.72	54.70	47.95
	5	61.62	89.35	71.40	73.05		5	42.57	47.82	47.65	55.57	49.28
	MVA	67.36	88.76	74.27	76.93		MVA	46.55	49.04	48.52	54.45	51.21
MCG	0.00	21.40	6.91	9.57	MCG	0.00	2.49	1.96	7.90	4.65		
CGS	0.00	4.31	2.31	2.13	CGS	0.00	2.35	1.63	3.40	1.11		
Imbalanced(0.8, 1)	1	92.77	90.23	89.87	93.80	Imbalanced(0.8, 1)	1	74.32	69.38	71.47	56.55	77.15
	2	56.85	90.33	60.77	63.02		2	52.95	56.08	52.80	56.92	57.10
	3	53.82	90.07	62.08	62.82		3	48.95	55.52	52.13	54.77	58.73
	4	58.00	90.15	61.52	63.35		4	48.40	54.97	52.40	55.33	57.93
	5	57.68	90.07	61.68	63.30		5	51.30	57.35	52.53	56.23	58.08
	MVA	63.82	90.17	67.18	69.26		MVA	55.18	58.66	56.27	55.96	61.80
MCG	0.00	26.35	3.36	5.44	MCG	0.00	3.48	1.08	0.78	6.62		
CGS	0.00	14.51	3.58	2.56	CGS	0.00	4.39	2.45	9.32	2.79		
Imbalanced(0.35, 2)	1	89.30	90.45	85.50	89.90	Imbalanced(0.35, 2)	1	69.43	66.38	64.22	63.10	74.13
	2	88.98	90.53	86.00	89.73		2	69.70	68.52	63.55	62.15	74.07
	3	69.07	89.83	73.97	75.35		3	45.17	62.18	53.70	60.58	64.93
	4	69.23	90.40	74.53	75.58		4	44.02	63.93	54.12	61.53	63.93
	5	69.53	90.48	73.55	75.02		5	47.12	64.37	56.98	62.60	64.23
	MVA	77.22	90.34	78.71	81.12		MVA	55.09	65.08	58.51	61.99	68.26
MCG	0.00	13.12	1.49	3.89	MCG	0.00	9.99	3.43	6.91	13.17		
CGS	0.00	9.61	4.01	2.65	CGS	0.00	9.95	7.46	11.34	7.12		
Imbalanced(0.6, 1)	1	92.27	90.38	89.25	92.80	Imbalanced(0.6, 1)	1	74.23	69.30	61.58	62.33	76.22
	2	68.65	90.73	71.58	71.80		2	45.08	65.70	49.05	61.43	64.17
	3	69.12	89.92	71.53	72.65		3	46.08	62.05	47.15	60.40	61.88
	4	68.78	89.33	72.85	73.45		4	43.80	63.97	48.67	60.53	59.10
	5	70.60	90.43	71.95	72.87		5	45.05	64.98	50.30	61.98	63.30
	MVA	73.88	90.16	75.43	76.72		MVA	50.85	65.20	51.35	61.34	64.93
MCG	0.00	16.28	1.55	2.83	MCG	0.00	14.35	0.50	10.49	14.08		
CGS	0.00	9.11	2.45	1.38	CGS	0.00	9.79	6.74	11.23	6.22		